The FPW Resonator Device Using PZT Sol-Gel Thin Film for Liquid Density Sensing

Jyh-Cheng YU* and Huang-Yao Lin
Department of Mechanical and Automation Engineering
National Kaohsiung First University of Science and Technology

Abstract

This paper presents the design, fabrication and preliminary results of a flexure plate wave (FPW) resonator using sol-gel derived lead zirconate titanates (PZT) thin films in the application of liquid density sensing. The propagation velocities of the FPW are very sensitive to the stress and the loading mass on the membrane. This research adopts the PZT thin films using Sol-Gel technique to fabricate the FPW resonator. The material system is Pt/Ti/PZT/LSMO/SiN_x. This study presents the simulation model for a two-port SAW resonator over a PZT substrate, which is extended to the design of the FPW resonator. The sensitivity of resonant frequency deviation will relate to the liquid density. The preliminary measurement results show that the resonant frequency and the non-viscous liquid density have a good linear correlation, and demonstrate the feasibility of the sensor application using the FPW resonator.

Keywords: FPW resonator, Flexure plate wave, PZT, Sol-Gel, Liquid density sensing

1. Introduction

Surface acoustic wave (SAW) can be generated by transferring the electronic signal through interdigital transducers (IDT) [1] to mechanical waves on the surface of a piezoelectric substrate. SAW is first discovered by Lord Rayleigh[2] in 1885 and thus called Rayleigh waves. The Rayleigh waves are the simplest guided waves whose energy is confined to within a wavelength and propagating on the surface. Recently, acoustic wave sensors have become popular applications in chemical sensors, pressure sensors, and accelerometers[3][4][5].

Lamb wave[6] are associated with Rayleigh waves on a thin plate whose thickness is smaller than the wavelength. They can be considered as two Rayleigh waves propagating on both sides of a plate. Two kinds of waves can propagate through the plate independently, namely the symmetric and the antisymmetric waves. The A_0 wave is the antisymmetric Lamb wave with the lowest velocity. The low operating frequency is an attractive feature as it implies relatively inexpensive associated electric circuit. This feature makes the wave suitable for liquid sensing due to the A_0 wave does not excite compressional waves in a loading liquid if its phase velocity is lower than the sound velocity of liquid. The back cavity of the FPW device can serve as the loading area of the sensing liquid.

Acoustic wave sensors used to be realized on a bulk piezoelectric substrate. Piezoelectric thin films, such as PZT, Zinc Oxide (ZnO), and Aluminum Nitride (AlN), have the cost advantage over crystal materials. Among them, the electromechanical coupling effect (K^2) of PZT is three to nine times and the dielectric constant 100 times over AlN and ZnO. Therefore, PZT is potentially suitable for thin film acoustic sensors.

In general, Lamb waves are propagating on the plate of finite thickness. Toda[7] propose the characteristics and the equivalent circuit model of delay line using Lamb wave. Jin and Joshi[8][9][10] derive the theoretical model for the propagation of the lowest-order symmetric (S_0) and the antisymmetric (A_0) Lamb wave modes on Y-Z lithium niobate. Also, due to the application potential of piezoelectric films, Jin and Joshi[11] present the excitation of ultrasonic Lamb wave by IDT in a composite plate consist of ZnO and SiN_x membrane, and compared with the theoretical calculations.

Lamb wave mode has a high mass sensitivity compared with other acoustic devices because of a thin plate. The change of properties of the acoustic wave due to the surface perturbation can be measured from the acoustic wave losses and frequency deviation using a network analyzer. Mass loading, damping, and mechanical loading cause the surface perturbation, and thus result in the shift of resonant frequency. Examples will be given of liquid sensing, viscosity sensing, fluid damping, mass loading sensing, pressure and vapor sensing.

Many researches address the application of Lamb wave sensors in chemical and liquid sensing. Laurent *et al.*[12] presented the theoretical modeling of FPW devices using AlN and ZnO, and compared with the experiments of liquid loading. Costello *et al.*[13] proposed the FPW device with ZnO for the viscosity sensing. The experimental results showed that the insertion loss increases and the resonant frequency reduces with the increase of the liquid viscosity. Weinberg *et al.*[14] derived the fluid-damping model of the FPW device with AlN. To increase the differentiability of the resonant frequency shift, reflecting gratings are added to the Lamb wave device

* 聯絡作者：jcyu@ccms.nkfust.edu.tw

that is first reported by Joshi[15]. The results showed that only a few strips of reflectors could achieve high reflection coefficient than a SAW resonator. Nakagwa [16] also adopted the same configuration but applied to a AT-cut quartz substrate.

This study will develop the FPW delay line and the FPW resonator using the structure of PZT on the silicon nitride membrane. We will discuss the design of the reflecting grating using the COM (Coupling of Modes) theory, and apply to the FPW devices. The liquid density will determine the non-viscous liquid loading when the device cavity is filled up with liquid. Finally, we will research the application feasibility of the FPW resonator for liquid density sensing.

2. The Fabrication of the FPW Resonator

Fig 1 shows the fabricating procedure of the FPW resonator that includes the coating of PZT film, the silicon etching, and the lift-off of IDT. The materials system consists of Pt/Ti/PZT/LSMO/SiN_x. First, we deposit the SiN_x (1.2μm) by LPCVD as the mask layer and the membrane structure on the (100) silicon substrate. Then the LSMO and the PZT thin films are multiple-coated by sol-gel techniques. The LSMO layer is used as a buffer layer between PZT and SiN_x to enhance the piezoelectric characteristic and avoid the crack of PZT. The electrode consists of Pt and Ti is patterned using lift-off techniques. Next, the back cavity is patterned on SiN_x using RIE. Finally, the membrane cavity of the device is fabricated using KOH anisotropic etching.

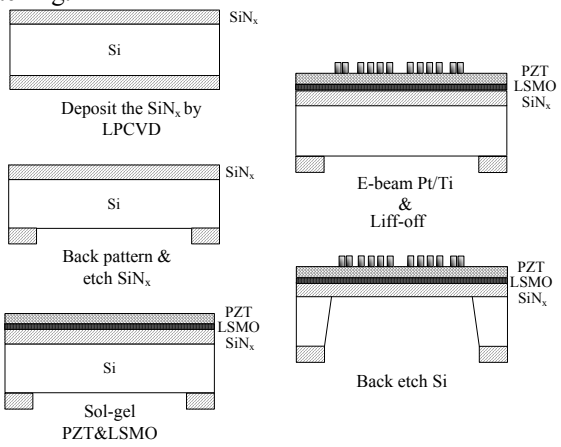

Fig 1 A schematic view of the fabricating process

3. The Modeling of SAW Resonators

SAW resonators can be represented by a set of transfer matrices from the COM theory. There are three basic elements on a typical SAW device: IDT, spacing, and reflector that can be described by three complex transmission matrices of [*T*], [*D*], and [*G*] respectively. Matrix [*T*] is a 3×3 transmission matrix for the IDTs, including both the acoustic and the electric parameters. Matrix [*D*] is a 2×2 matrix for the acoustic transmission line between IDTs and gratings. Matrix [*G*] is a 2×2 matrix for the SAW reflection grating to describe the relationship between the acoustic transmission and reflection response[17].

3.1. Overall acoustic matrix [*M*] for the two-port SAW resonator

As shown in Fig 2, the overall acoustic matrix for the two-port resonator is obtained from the product of the composite building blocks that consist of the reflection grating, IDT's, and the delay lines. Here, G_1 and G_7 are relating to the SAW reflection gratings. D_2 and D_6 are the delay line matrices for the spacing between the gratings and adjacent IDTs, while D_4 is the transmission matrix for the separation between IDTs. T_3 and T_5 are the IDT transmission matrices. The terms, *a* and *b* of T_3 and T_5, represent the incident and the reflected electrical signals respectively.

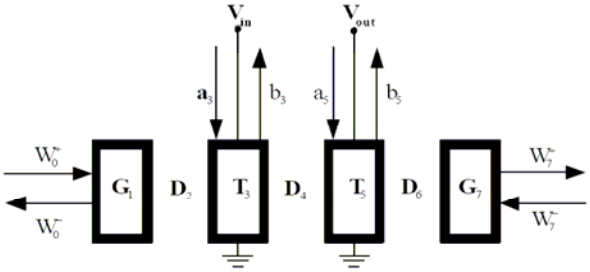

Fig 2 Representation of two-port resonator building blocks

If there is no input electrical signal for the output IDT, $a_5 = 0$, the overall acoustic modeling can be simplified as follows:

$$[W_0] = [M][W_7] + a_3[G_1][D_2][\tau_3] \quad (1)$$

where $[M] = [G_1][D_2][T_3][D_4][T_5][D_6][G_7]$

τ_3 is the column matrix relating to the input coupling.

Assume an absorber is applied to the outside of the reflection grating; there will be no incident acoustic wave for the gratings G_1 and G_7.

$$W_0^+ = W_7^- = 0 \quad (2)$$

Substituting the boundary conditions to Eq. (1), we can obtain

$$\begin{bmatrix} 0 \\ W_0^- \end{bmatrix} = [M]\begin{bmatrix} W_7^+ \\ 0 \end{bmatrix} + a_3[G_1][D_2][\tau_3] \quad (3)$$

From transmission matrices of Fig 2, the b_5 is given by

$$b_5 = [\tau_5'] \cdot [W_5] \quad (4)$$

where τ_5' is a column vector relating to the output coupling

The transmission coefficient is then as follows:

$$S_{21}\big|_{a_5=0} = b_5 / a_3 \qquad (5)$$

3.2. Two-port SAW resonator simulation

This section will simulate the two-port SAW resonator over a bulk PZT using COM model. The simulation parameters used here are: acoustic wavelength is 40 (μm) with uniform finger spacing, separation between IDTs = 10 wavelengths, and the phase velocity of bulk PZT is 2400 (m/s). The reflection phase, θ, is determined by the position of standing wave at the reference plane relating the sign of reflected-to-incident surface waves entering the reflection grating, which will affect the spacing design between the gratings and adjacent IDTs (D_2 and D_6). This determination of reflecting phase is difficult and often depends on the experimental for the material combination of the piezoelectric substrate and the reflecting electrodes[17]. The reflection coefficient for the PZT thin film and Pt/Ti reflecting grid is not available and will depend on future experimental. However, since PZT is a strong piezoelectric, similar to lithium niobate, the reference phase $\theta = 0^{\circ}$ for the open circuit design of reflector

Based on the above assumption, we then determine the design parameters for the two-port resonator.

(1) The number of reflection grating is 40 that are to form standing waves to reduce insertion loss.
(2) The number of pairs of IDT is 20.
(3) The overlap length of IDT is 50λ because it has a low insertion loss and high transmission effect.
(4) The spacing between the gratings and adjacent IDTs ($D2$) are $(1/8+n/2)\lambda$, and the separation between the IDTs is 10λ.

Fig 3 shows the simulation result of the proposed design. The resonator design will be applied to FPW, but the resonant frequency will be determined by the phase velocity of FPW.

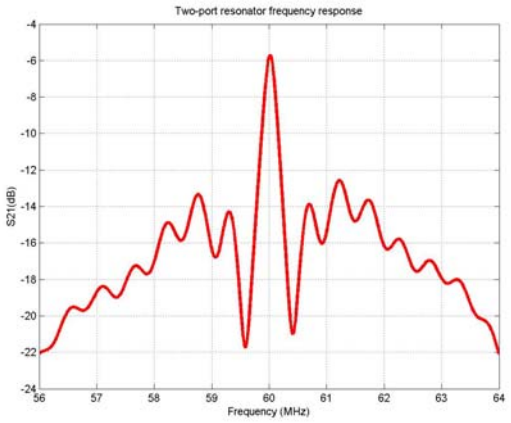

Fig 3 Two-port saw resonator frequency response

4. The Modeling of FPW Wave Sensors

4.1. The phase velocity of FPW

Consider the A_0 mode of FPW propagating on a thin plate; the phase velocity of the plate regime can be expressed as [18] [19]:

$$v_P = \left(\frac{B}{M}\right)^{1/2} \qquad (6)$$

where $B = \left(\frac{\lambda}{2\pi}\right)^2 \frac{E' d^3}{12}$ is the bending stiffness of a homogeneous isotropic plate

$E' = E/(1-\upsilon^2)$ is the effective Young's modulus,

E is actual Young's modulus,

ν is the Poisson's ratio,

d is the plate thickness, and

M is the mass per unit area of the plate.

The phase velocity of the plate regime subject to a tensile stress and liquid loading can be well approximated by the simple asymptotic expression:

$$v_P = \left(\frac{T_x + B}{M + \rho_F \delta_E + M_\eta}\right)^{1/2} \qquad (7)$$

where T_x is the component of in-plane tension in the x direction,

$\rho_F \delta_E$ is the mass effect,

ρ_F is the density of the fluid, and

M_η is the viscosity effect.

$$\delta_E = \left(\frac{\lambda}{2\pi}\right)\left[\left(1 - \frac{v_P}{v_F}\right)^2\right]^{-1/2} \qquad (8)$$

$$M_\eta = \frac{\rho_F \delta_V}{2} \qquad (9)$$

where $\delta_V = \left(\frac{2\eta}{\omega \rho_F}\right)^{1/2}$ is the viscous decay length,

ω is the operating angular frequency, and

η is the shear viscosity.

4.1.1. Effects of the loading with a non-viscous liquid on the plate

When the FPW device is in contact with a loading liquid, the phase velocity will be influenced by the mass effect ($\rho_F \delta_E$) that can be determined by the evanescent decay length. If the acoustic velocities of the plate, v_p, is much smaller than the fluid velocity, v_F, the term in the brackets of Eq.(8) is approximate unity. The effective evanescent decay length, δ_E, is about $\lambda / 2\pi$.

When the liquid thickness is larger than the evanescent decay length, the mass-loading effect of the liquid will remain the same as shown in Fig 4. The mass sensitivity and tension sensitivity of the perturbation of phase velocity are as follows:

$$\frac{\Delta v_p}{v_p} = s_m \times \rho_F + s_T \times T_x \qquad (10)$$

where $s_m = -\dfrac{\delta_E}{2(M + \rho_F \delta_E)}$, $s_T = \dfrac{1}{2(T_x + B)}$

In our case, s_m =-2.78(m^2/N) and s_T =7.69*10-5(m/N). The tension effect due to the liquid pressure can be ignored when compared with the bending stiffness. Therefore, when the device cavity is filled up with different liquids, the change of the phase velocity will be related to the density of the liquid and thus can be used as a density sensor.

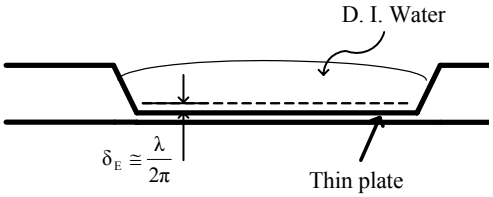

Fig 4 The evanescent decay length for the liquid loading in a FPW device

4.1.2. Effects of the loading with a viscous liquid on the plate

The viscosity effect for a viscous liquid can be estimated by adding an effective mass-loading term, M_η in addition to the mass effect ($\rho_F \delta_E$). From Eq.(7), we know that the phase velocity of FPW will be influenced by fluid density (ρ_F) and shear viscosity (η) of the loading liquid. However, we can't differentiate the velocity perturbations between liquid density and viscosity because the density and viscosity are coupled in the viscous effect as seen from Eq. (9). In another word, the liquid viscosity can't be determined by the frequency shift. Thus, we focus on the density sensing for non-viscous liquids in the following study. However, we will also study the viscosity effect by comparing two different liquids with the same density.

4.2. The estimate of the phase velocity of the device

The material structure of the proposed FPW device is Pt (0.15μm)/Ti (0.02 μm)/PZT(1 μm)/LSMO (0.1 μm)/SiN_x (1.2 μm). Table 1 lists mechanical properties of the material system. The PZT properties are assumed from bulk material. Also, the material properties of LSMO are not available and assumed to be the same as the PZT film. The mass effect of the Pt and the Ti are assumed negligible.

Table 1 The material properties of the composite plate

	SiN_x	PZT (PZT + LSMO)	Ref.
Thickness (μm)	1.2	1.1 (1 PZT+0.1 LSMO)	
Young's modulus (E, N/m^2)	3.85*10^{11}	8.6*10^{10}	[20]
Poisson ratio (v)	0.27	0.25	
Density (ρ, kg/m^3)	3100	7600	
M (kg/m^2)	0.00372	0.00836	

4.2.1. The phase velocity of the device in air

The thickness of the composite plate is 2.3 (μm). The material parameters of the membrane can be estimated from the composite plate theory as shown in Table 2.

The wavelength of the FPW is determined by the period of IDT which is selected to be 40 (μm). The phase velocity is 235.06 (m/s) from Eq.(7), and the resonant frequency of the device in air will be f_{air} = 5.88 (MHz).

Table 2 The parameters of the composite plate

E	2.42*1011 (N/m^2)
M	0.1176 (N/m^2)
v	0.26
E'	2.6*1011 (N/m^2)
B	6497.93 (N/m)

4.2.2. The phase velocity for the device loaded with non-viscous liquids

When water is dripped on the thin plate, the loading will induce the added-mass and the tension effects. The weight of the water filled in the cavity is about 0.0056 (g) that can be estimated form the multiplication of the water density (ρ), the plate area (A), and the depth of the membrane cavity (H). Since the acoustic velocity of water is 1480 (m/s) that is much smaller than $v_{p(air)}$ = 235.06 (m/s), the effective evanescent decay length, δ_E, is about $\lambda / 2\pi$. By substitute the parameters in to Eq. (7), we can obtain the phase velocity for the FPW device loaded with non-viscous liquids as shown in Table 3.

Table 3 Estimated resonant frequency of the FPW device loaded with non-viscous liquids

	IPA	Water	Saline solution
Phase Velocity (m/s)	197.48	190.05	183.77
Resonant Frequency (MHz)	4.94	4.75	4.59

4.2.3. The phase velocity for the device loaded with glycerol

When a viscous liquid is dripped on the thin plate, the loading will induce an additional viscosity effect as shown in Eq. (7). Here, we prepare a saline solution with the same density as glycerol to analyze the additional viscosity effect. From the estimation results as shown in Table 4, the viscosity effect of glycerol will introduce an additional deviation of 0.1 (MHz) for the resonant frequency.

Table 4 The resonant frequencies of the glycerol and the saline solution with the same density

	Saline solution	Glycerol
Phase Velocity (m/s)	183.77	179.58
Resonant Frequency (MHz)	4.59	4.49

5. Experimental Results and Discussions

5.1. The FPW delay line and the FPW resonator signals

The frequency responses of the FPW delay line and the FPW resonator are shown in Fig 5. From the analysis in section 4.2, the calculated resonant frequency of the A_0 mode is about 5.88 (MHz) that is close to the experimental results for the FPW delay line of 5.47 and the FPW resonator of 5.53 (MHz). The difference between the theoretical and experimental results might be due to the application of the material properties of bulk PZT in the estimation because the film properties are not available. As expected, the FPW resonator (-16.5 dB) has a lower insertion loss than the FPW delay line (-23.4 dB).

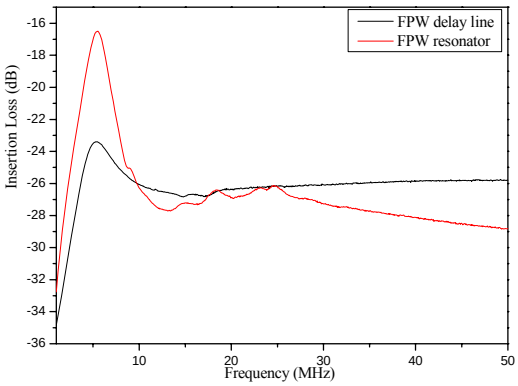

Fig 5 The S_{21} frequency response of the FPW devices

5.2. Liquid sensing using the FPW delay line and the FPW resonator

5.2.1. The density sensing for non-viscous liquids

The sensitivity analysis between the resonant frequency and the densities for non-viscous liquids is summarized in Fig 6. The resonant frequency decreases as the liquid density increases due to the mass effect. The results show that the resonant frequency and the liquid density have a good linear correlation despite a static difference, which demonstrates the feasibility of density sensing. The static difference may be due to liquid damping and stress effects that are presumed negligible. Also, the material properties of the piezoelectric thin film might be different from the bulk material properties used in the theoretical estimation. Detailed explanations are pending future investigation.

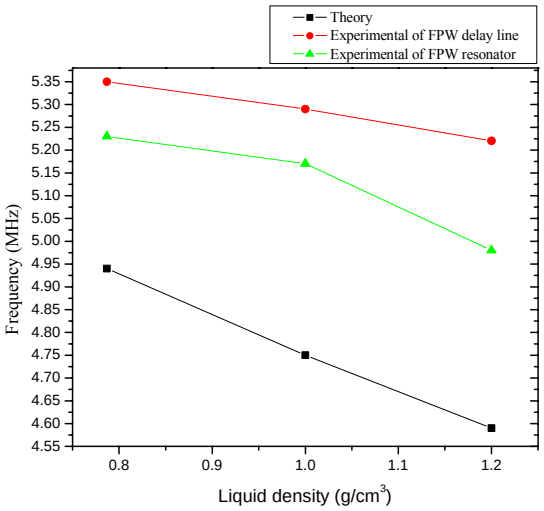

Fig 6 The sensitivity analysis between the resonant frequency and the density for non-viscous liquids

5.2.2. The frequency deviation due to liquid viscosity

When the plate is loaded with viscous liquids, the decay of the propagation is caused by energy radiation of liquid and energy loss from the friction effect on the solid-liquid interfaces. When a viscous liquid, such as glycerol, is dripped on the thin plate, the loading will induce an additional viscosity effect as shown in Eq.(7). Here, we compare two liquids, glycerol and saline solution with the same density to study the viscosity effect. From Table 5, we observe that the glycerol loading will introduce additional frequency deviation compared with the saline solution with the same density. Also, the viscosity effect of glycerol will cause more damping effect than the saline solution and increases the insertion loss.

Table 5 The comparison between viscous and non-viscous liquids with the same density

	Theoretical	Experimental	
	Frequency (MHz)	Frequency (MHz)	Insertion Loss (dB)
Saline solution	4.59	4.98	-33.38
Glycerol	4.49	4.73	-37.04

6. Conclusions

This study has successfully fabricated the FPW resonator on the PZT piezoelectric thin films and compared with the modeling analysis. The device is applied to the loading of non-viscous and viscous liquids. We have observed that the liquid loading will increase the insertion loss and decrease the resonant frequency that is consistent with theoretical prediction. Three non-viscous liquids, DI Water, IPA and saline solution, are applied to the resonator. The results show that the resonant frequency and the liquid density have a good linear correlation despite a static difference, which

demonstrates the feasibility of density sensing. To study the viscosity effect, two liquids, glycerol and saline solution with the same density are investigated. Additional frequency deviation is observed and the insertion loss is increased for viscous liquid (glycerol), which also matches fairly with the theoretical estimation.

7. References

[1]. White, R. M. and Voltermer, F. W., Direct piezoelectric coupling to surface elastic wave, Applied Physics Letter, Vol. 7, pp. 314-316, 1965
[2]. Rayleigh, L.,On waves propagated along the plane surface of an elastic solid, Proc. London Math. Soc., Vol. 17, pp. 4-11, 1885
[3]. Yakovkin,L. et al., Highly sensitive SAW sensors, Proceedings of IEEE International Frequency Control Synposium, pp. 395-400,1994.
[4]. Galipeau, D. W. et al., Surface acoustic wave microsensors and applications, Smart Material Structure, Vol. 6, pp. 658, 1997
[5]. Drafts, B., Acoustic wave technology sensors, IEEE Transactions on Microwave Theory and techniques, Vol. 49, No. 4, pp. 795-802, 2001
[6]. Vellekoop, M. J., Acoustic wave sensors and their technology, Ultrasonic, Vol.36, pp. 7-14, 1998
[7]. Toda, K., Lamb-wave delay lines with interdigital electrodes, Japanese Journal of Applied Physics, Vol. 44, pp. 56-62, 1973
[8]. Jin, Y. and Joshi, S. G., Excitation of ultrasonic Lamb wave in piezoelectric plates, Japanese Journal of Applied Physics, Vol. 69, pp. 8018-8024, 1991
[9]. Jin, Y. and Joshi, S. G., Propagation of ultrasonic Lamb waves in piezoelectric plates, Japanese Journal of Applied Physics, Vol. 70, pp. 4113-4120, 1991
[10]. Jin, Y. and Joshi, S. G., Lamb wave propagation in piezoelectric plates, Ultrasonics Symposium, pp. 1023-1027,1991
[11]. Jin, Y. and Joshi, S. G., Excitation of ultrasonic Lamb waves in composite membranes, Ultrasonics Symposium, pp. 429-432, 1995
[12]. Laurent, T., Lamb wave and plate mode in ZnO/silicon and AlN/silicon membrane Application to sensors able to operate in contact with liquid, Sensors and Actuators, pp. 26-37, 2000
[13]. Costello, B. J., Ultrasonic plate waves for biochemical measurements, Ultrasonics Symposium, pp. 977-981, 1989
[14]. Weinberg, M. S., Fluid damping in resonant flexural plate wave device, Journal of Microelectromechanical Systems, Vol. 12, No. 5, pp. 567-576, 2003
[15]. Joshi, S. G. and Zaitsev, B. D., Reflection of ultrasonic Lamb waves propagating in thin piezoelectric plates, Ultrasonics Symposium, pp.423-426, 1998
[16]. Nakagwa, Y., Momose, M. and Kakio, S., Characteristics of reflection of resonators using Lamb wave on AT- cut quartz, Japanese Journal of Applied Physics, Vol. 43, pp. 3020-3023, 2004
[17]. Campbell, C. K., Surface acoustic wave devices for mobile and wireless Communications, San Diego: Academic Press, 1998
[18]. Wenzel, S. W. and White, R. M., A multisensor employing an ultrasonic Lamb-wave oscillator, IEEE Transactions Electron Devices, Vol. 35, 1998
[19]. White, R. M. et al., Acoustic Wave Sensors Theory, Design, and Physico-Chemical Applications, Academic Press, 1996
[20]. http://www.piezo-kinetics.com/PKI_700.htm

鋯鈦酸鉛薄膜撓性板波共振元件於液體感測之研究

*余志成[1]　林煌堯[2]
國立高雄第一科技大學
機械與自動化工程研究所

摘要

本論文探討鋯鈦酸鉛（PZT）壓電薄膜於撓性板波（FPW）共振元件之液體感測應用。撓性板波傳遞速度對外界干擾的物理量如應力、質量等，具有相當的敏感度。且當聲波在與液體接觸時，其波傳能量不易散射出去。而撓性板波其背部薄膜孔穴可作為待測溶液的負載區，可精確檢驗出傳遞基材受外界激發所產生的薄板負載質量與應力的變化，故適於液體感測之應用。本研究主要以溶膠-凝膠法製備鋯鈦酸鉛壓電薄膜，來進行撓性板波共振元件製作。元件的材料系統為 Pt (0.15μm)/Ti (0.02 μm)/PZT(1 μm)/LSMO (0.1 μm)/SiN_x (1.2 μm)。在理論分析方面利用反射柵欄特點並結合撓性板波的波傳特性來製造撓性板波共振元件。並實際將該元件應用於液體密度感測，結果顯示元件的插入損失和共振頻率會隨著液體負載密度的大小呈線性變化。而該元件的設計比一般撓性板波元件有更低的插入損失值，驗證了本元件於液體感測應用的可行性。

關鍵字：撓性板波共振器、撓性板波、鋯鈦酸鉛薄膜、溶膠-凝膠法、液體密度感測